ELSEVIER

International Journal of Applied Earth Observation and Geoinformation xxx (2003) xxx–xxx

INTERNATIONAL JOURNAL OF APPLIED EARTH OBSERVATION AND GEOINFORMATION

www.elsevier.com/locate/jag

A Multiscale Object-Specific Approach to Digital Change Detection

Ola Hall [a,*], Geoffrey J. Hay [b]

[a] *Department of Physical Geography and Quaternary Geology, Stockholm University, SE-106 91 Stockholm, Sweden*
[b] *Geocomputing Laboratory, Département de Géographie, Université de Montréal, C.P. 6128, Succursale Centre-Ville, Montréal, Qué., Canada H3C 3J7*

Received 20 December 2002; accepted 16 May 2003

Abstract

Landscape spatial pattern is dependent not only on interacting physiographic and physiological processes, but also on the temporal and spatial scales at which the resulting patterns are assessed. To detect significant spatial changes occurring through space and time three fundamental components are required. First, a multiscale dataset must be generated. Second, a change detection framework must be applied to the multiscale dataset. Third, a procedure must be developed to delineate individual image-objects and identify them as they change through scale. In this paper, we introduce an object-specific multiscale digital change detection approach. This approach incorporates multitemporal SPOT Panchromatic (Pan) data, object-specific analysis (OSA), object-specific up-scaling (OSU), marker-controlled watershed segmentation (MCS) and image differencing change detection. By applying this framework to SPOT Pan data, image-objects that have changed between registration dates can be identified and delineated at their characteristic scale of expression. Results illustrate that this approach has the ability to automatically detect changes at multiple scales as well as suppress sensor related noise. This study was conducted in the forest region of the Örebro Administrative Province, Sweden.

Keywords: Digital change detection; Multiscale object-specific analysis; Watershed transformation; Remote sensing; SPOT; Hierarchy; Scale domain; Image differencing; Multiscale; Critical landscape threshold

1. Introduction

Ecological theory, in particular hierarchy theory (Allen and Starr, 1982), predicts that changes in landscape spatial pattern and structure are dependent on the spatial and temporal scales at which they are assessed (Meentemeyer and Box, 1987; Turner, 1989; Malingreau and Belward, 1992). This theory also predicts that landscapes are composed of separated levels (*scale domains*). Scale domains are separated by *scale thresholds*, which represent a break in the relative importance of process variables (Meentemeyer, 1989; Wiens, 1989). Therefore, any methodological framework for analyzing landscape change needs the capacity to explicitly handle scale. In general terms, 'scale' corresponds to a 'window of perception'. As the size (i.e. grain and extent) of the window is changed, new patterns and structures emerge; thus, the conclusions drawn by the observer are strongly influenced by the scale of observation. The term 'grain' refers to the smallest distinguishable component, i.e. spatial resolution,

* Corresponding author. Tel.: +46-8-6747852; fax: +46-8-169629.
E-mail address: ola.hall@humangeo.su.se (O. Hall).

0303-2434/03/$ – see front matter © 2003 Elsevier B.V. All rights reserved.
doi:10.1016/S0303-2434(03)00010-2

while 'extent' refers to the total area or time under analysis.

To detect changes at different scales within the landscape, three fundamental components are required:

1. a multiscale data source,
2. a change detection framework, and
3. feature detectors that can detect relevant changes at specific scales.

A number of computational techniques currently exist that allow for multiscale representations (Starck et al., 1998). Among the most common are, fractals (Mandelbrot, 1967), quadtrees (Klinger, 1971), pyramids (Klinger and Dyer, 1976; Serra, 1988), wavelets (Daubechies, 1988; Hu et al., 1998), Fourier transforms (Townshend and Justice, 1988) and scale space (Lindeberg, 1994; Hay et al., 2002). A more recent addition that exhibits novel characteristics important for multiscale landscape analysis is referred to as multiscale object-specific analysis (MOSA) (Hay et al., 2003):

- The MOSA framework has been developed for the specific spatial sampling context provided by remote sensing imagery where it explicitly considers pixels as parts of objects that exist at different scales, thereby addressing the hierarchical structure of landscapes (Hay et al., 1997).
- Objects rather than arbitrarily selected pixels are the basis for up-scaling (i.e. re-sampling to coarser scales), thus the effects of the modifiable areal unit problem (MAUP) are reduced (Openshaw, 1984; for a comprehensive review of MAUP, see Marceau, 1999 and Marceau and Hay, 1999).
- This framework automatically identifies significant *scale domains* and generates multiscale datasets based on the spatial attributes of the varied sized, shaped and spatially distributed objects composing an image (Hay et al., 2001).
- MOSA incorporates an object-based mechanism for automatic multiscale feature detection (Hall, 2002; Hall et al., 2003), so that objects can be topologically linked and queried through scale (Hay et al., 2002).

Digital change detection is the computerized process of identifying changes in the state of an object, or other earth-surface features, between different dates (Singh, 1989). The underlying premise for using remote sensing data is that a change in the status of an object must result in a change in radiance values. However, variables such as atmospheric condition, solar angles, misregistration, and phenology reduce the 'signal-to-noise ratio'. Calibrating for these exogenous effects is a non-trivial task (Schott et al., 1988; Dai and Khorram, 1998).

During the last three decades, a large number of change detection methods have evolved that differ widely in refinement, robustness and complexity. Therefore, Deer (1998) suggested a three level categorization system that differentiates these methods by introducing the notion of *pixel*, *feature*, and *object* level image processing. In Table 1, we provide a summary of surveyed methods that are arranged according to Deer's categorization system. Within these categories, *pixel level* refers to numerical values of each image band, or simple calculations between corresponding bands such as image differencing or rationing. In general, it is not possible to attach any symbolic meaning (e.g. a decrease in total forest canopy) from the pixel level without further analysis. The *feature level* is a more advanced level of processing, which involves transforming the spectral or spatial properties of the image (e.g. principal components analysis (PCA), texture analysis, or vegetation indices), thus the enhanced feature may have real-world meaning (e.g. vegetation indices in the radiometric domain, or lines/edges in the spatial domain) or may not (e.g. principal components in the radiometric domain). The *object* is the most advanced level of processing. All levels can involve symbolic identification in addition to pixel or feature change detection. The general approach to symbolic identification is to compare two classifications pixel-by-pixel. Although, the most complete approach, it generally results in low change detection accuracy (Singh, 1989).

Recent advances in digital change detection also involve multiresolution approaches. Carvalho et al. (2001) applied a multiresolution wavelet transform to multitemporal and multiresolution Landsat (TM and MSS) data with the objective to reduce radiometric and geometric misregistration, and to incorporate images with different spatial resolution. The underlying assumption was that 'noise' and 'signals' would be sorted according to magnitude and frequency. They found the method insensitive to misregistration (i.e. geometric and radiometric) and noted that changes

Table 1
Summary of main digital change detection methods

Method	Author	Level
Change vector analysis	Malila (1980), Virag and Colwell (1987), Lambin and Strahler (1994), Lambin (1996) and Johnson and Kasischke (1998)	Pixel
Endmember analysis	Adams et al. (1995) and Kressler and Steinnocher (1999)	
Image differencing	Weismiller et al. (1977), Singh (1986), Gong et al. (1992) and Manavalan et al. (1995)	
Image rationing	Todd (1977)	
Image regression	Singh (1986), Hanaizumi et al. (1991) and Jha and Unni (1994)	
Local texture	Lazaroff and Brennan (1992)	Feature
Principal components analysis	Lodwick (1979), Byrne et al. (1980), Singh and Harrison (1985), Fung and LeDrew (1987), Deer and Longmore (1994), Siljeström Ribed and Moreno Lópes (1995) and Collins and Woodcock (1996)	
Shape analysis	Choo et al. (1989)	
Vegetation index differencing	Coiner (1980), Nelson (1983), Coppin and Bauer (1994) and Lyon et al. (1998)	
Wavelet	Carvalho et al. (2001) and Collins and Woodcock (1994)	
Artificial intelligence	Matsuyama (1987)	Object
Artificial neural networks	Gopal and Woodcock (1996), Dai and Khorram (1997) and Chan et al. (2001)	
Direct multidate classification	Weismiller et al. (1977) and Hoffer and Lee (1989)	
Expert system	Stefanov et al. (2001)	
Fuzzy post-classification comparison	Fisher and Pathirana (1993), Deer (1998), Eklund et al. (2000), Deer and Eklund (2001) and Foody (2001)	
Post-classification comparison	Gordon (1980), Riordan (1980), Jensen et al. (1995) and Munyati (2000)	

were well discriminated according to their assumptions. In fact, the result of this technique resembles PCA as performed by Fung and LeDrew (1987) and Collins and Woodcock (1996). PCA is known to account for exogenous signal characteristics, such as differences in illumination and atmospheric conditions. Based upon the preceding information, the primary objective of this study was to apply MOSA (Hall, 2002; Hay et al., 2003) to automatically detect landscape changes at their characteristic scales of expression. MOSA was applied to only one channel (i.e. Panchromatic (Pan)) of the multispectral SPOT (Satellite Pour l'Observation de la Terra) dataset in order to reduce the number of resulting image-sets, which increase dramatically with the inclusion of additional channels (cf. Hall, 2002). Thus, a change detection framework is suggested with feature level capabilities that can be extended to the object level with the addition of a standard classification algorithm. More generally, this study also aims at addressing four recent issues in remote sensing based landscape analysis:

1. The problem of how to integrate the dynamics of change across space from detailed to broad scales (Holling et al., 2002).
2. The automatic delineation of the varying sized, shaped, and spatially distributed objects within a

landscape at their characteristic scales of expression (Hay et al., 1996, 1997).
3. The use of multiscale techniques to evaluate how landscape objects evolve through scale (Hay et al., 2002; Turner et al., 2001).
4. The meaningful characterization of landscape pattern dynamics (Turner, 1989; Lambin, 1996).

2. Study site and dataset

2.1. Study site

The study site is located within the Örebro Administrative Province, Sweden (Fig. 1a). The region as a whole is part of the southern boreal zone, which is dominated by coniferous forest and the sporadic occurrence of nemoral trees. Species of Aspen (*Populus tremula*) and Birch (*Betula pendula*, *B. pubescens*) are common throughout the region and fens and bogs occur frequently within the study site. A number of glaciofluvial deposits can also be found near the frequently occurring lakes and streams. Sandy till dominates the area. This site is located approximately 150–210 m above sea level. Agriculture has never been an important activity in the study area. Instead, the many lakes and streams have given rise to an early mining industry though today, forestry is dominant (Jansson, 2001). Settlement is sparse throughout the area.

2.2. Data

Two 10 m, single channel Pan SPOT (2 and 3) scenes with a spatial extent of 60 km × 60 km were acquired over this area on 27 May 1992 and 17 September 1996. Geometric rectification was performed at the receiving station according to an orbital model and digital elevation data (see Table 2 for details on data acquisition). For this study, a 10 km × 10 km (1000 × 1000 pixels) subset was extracted from the original scenes. In the following sections, the notation Pan_1 refers to the subset from 1992, and Pan_2 refers to the subset from 1996.

In each Pan sub-image, black is associated with water bodies, dark tones with forest, gray tones with forest clearings and bright tones with constructed objects such as roads or buildings. A power-line transects the study site diagonally from west to east, running almost parallel with the only major road in this area. Upon an initial visual assessment, Pan_1 (Fig. 2a) and Pan_2 (Fig. 2b) appear very similar. However, a more detailed visual examination reveals two distinct types of differences. First, we note that there are structural changes in the landscape that have occurred between 1992 and 1996 that are related to new forest clearings, re-growth

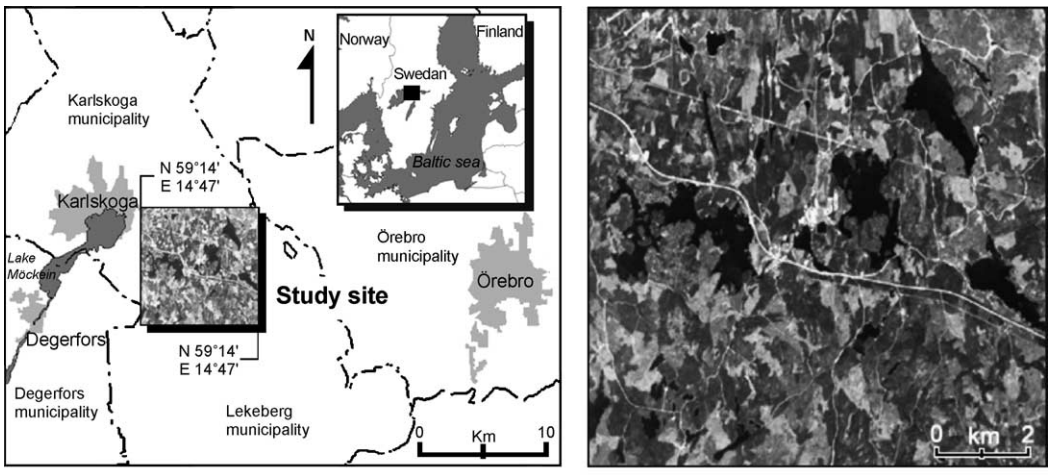

Fig. 1. Study site map (a) and SPOT image overview (b).

Table 2
Image acquisition properties

Property	Pan_1	Pan_2
Receiving station	Kiruna	Kiruna
Scene identity/date	054229/920527	054229/960917
Mission	SPOT-2	SPOT-3
Instrument	HRV1	HRV1
Mode	PAN	PAN
Viewing angle (°)	−23.54	−0.13
Overpass	10:01:20	10:28:33
Sun azimuth (°)	159.67	172.92
Sun elevation (°)	50.86	32.66
Nominal resolution (m)	10	10
No. of ground control points	23	10
RMS (m)	4.04	6.88
Wavelength (μm)	0.50–0.72	0.50–0.72
Number of bits	8	8

of forest vegetation, and the construction of minor roads. Second, there are 'image' changes that are due to differences in sensor-target-illumination, viewing angle, and solar azimuth (confirmed in Table 2). These changes can be observed where roads pass through tall forest stands, resulting in roads being 'shadowed' in one image but not in the other. In addition, the length and direction of shadows will appear different in both scenes. We also note a difference in overall image contrast between the two scenes, which in Fig. 2 have been contrast normalized (see Section 3 for details).

3. Methods

Data analysis was conducted in four steps:

1. radiometric normalization,
2. object-specific multiscale dataset generation using object-specific analysis (OSA) and object-specific up-scaling (OSU),
3. feature detection using marker controlled segmentation (MCS), and
4. change detection.

Normalization and image analysis were performed using ENVI 3.5 (http://www.rsinc.com/envi/). MOSA was developed in IDL 5.5 (http://www.rsinc.com/idl/); and MCS and change detection were written in Matlab 6.1 (http://www.mathworks.com).

3.1. Normalization

Change detection is highly dependent on accurate geometric and radiometric correction (Schott et al., 1988; Dai and Khorram, 1998; Carvalho et al., 2001). In this study, geometric rectification was performed at the Kiruna receiving station (see Section 2), however, radiometric correction was performed by the authors, and is described as follows.

When a comparison of surface reflectance is not important, Song et al. (2001) show that a relative calibration is sufficient. Relative calibration involves

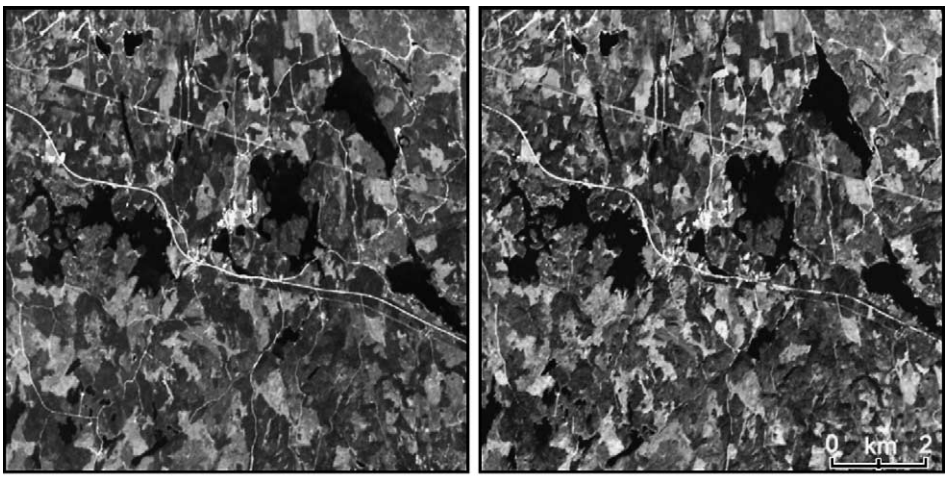

Fig. 2. Radiometric normalized SPOT Panchromatic image set. Reference image Pan_1 (a) and subject image Pan_2 (b).

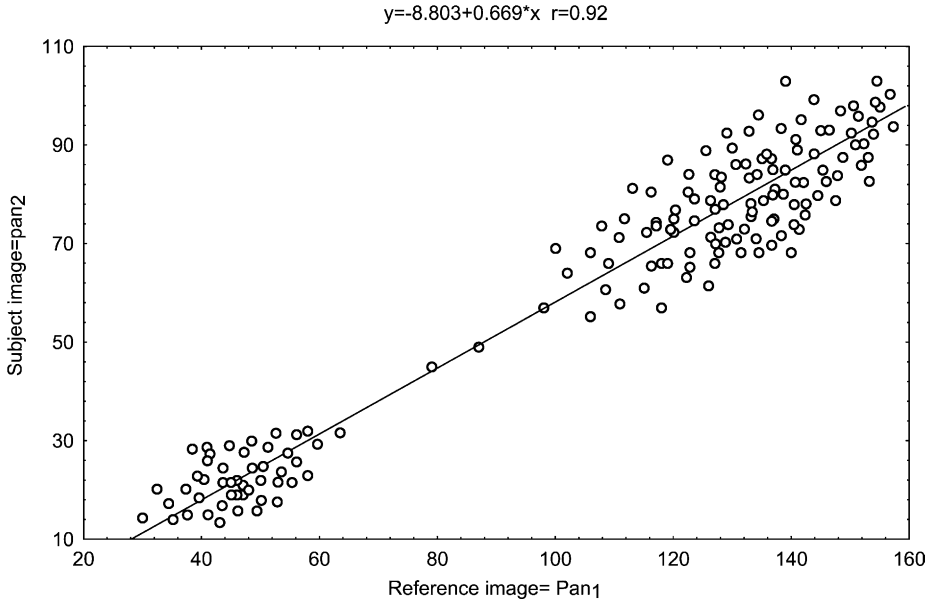

Fig. 3. Linear relationship between pseudo-invariant features.

normalizing the digital numbers (DN) of multitemporal images to a reference image, the underlying assumption being that there exists a linear relationship between images across time (Song et al., 2001).

Schott et al. (1988) have developed a normalization method based on pseudo-invariant features (PIFs). PIFs are objects with nearly invariant reflectivity across time. These are typically constructed objects whose reflectance is independent of seasonal or biological cycles, and that are spatially well defined (i.e. urban features such as buildings and roads). Coppin and Bauer (1994) have extended the list of PIFs by using a dense mature even-aged homogeneous red pine stand and a deep lake. Differences in the brightness distribution of the invariant features are assumed to be a linear function. The PIF method does not decrease the magnitude of change between scenes (Yang and Lo, 2000).

In this study, we applied relative calibration based on 121 sampled PIFs (i.e. lakes and roads) that were selected from a visual inspection of Pan_1 and Pan_2. Pan_1 was used as the reference image. The linear relationship between PIFs from the two images was, $Pan_2 = -8.803 + 0.669 \times Pan_1$, $r = 0.92$. All pixels in Pan_2 were normalized according to this linear relationship, which is illustrated in Fig. 3.

3.2. Generating a multiscale dataset

MOSA is composed of three primary components: *object-specific analysis* (OSA), *object-specific up-scaling* (OSU), and *marker-controlled watershed segmentation* (MCS). OSA is a multiscale approach that automatically defines unique spatial measures specific to the individual image-objects composing a remote sensing scene (Hay et al., 1997, 2001). These object-specific measures are then used in a weighting function (OSU) that automatically up-scales an image to a coarser spatial resolution, by taking into account the spatial influence of the image-objects composing the scene at a finer spatial resolution. Then MCS is applied to these up-scaled data to automatically segment them into topologically discrete image-objects that correspond to visually defined image-objects (Hall et al., 2003).

The term ‘image-object’ (Hay and Niemann, 1994) refers to individually resolvable entities located within a digital image that are perceptually generated from high-resolution pixel groups. *High-resolution*

corresponds to a situation where real-world objects are modeled by many individual pixels (Woodcock and Strahler, 1987). The term *low-resolution* represents the spectral integration of many (smaller) real-world objects within a single pixel. As a result, an image-object tends to be composed of spatially clustered pixels with high autocorrelation because they are part of the same object (Hay et al., 2002). In a satellite sensor image, each pixel exhibits both high- and low-resolution duality.

An underlying premise of OSA/OSU is that all pixels are exclusively considered as high-resolution. Thus pixels are used to define the size of the image-object they are part of. In practice, this is done by evaluating the variance within an iteratively growing window centered over each pixel until a series of heuristics are met (see Hay et al., 2001 for details). Based on these heuristics, a threshold is defined as the kernel reaches the image-object's edges. The window size at this location corresponds to the objects known size. When this threshold is reached, corresponding mean and variance values are recorded for the pixel under analysis. This process is repeated for all pixels within the original image, resulting in corresponding variance (V_1), area (A_1), and mean (M_1) images. This constitutes OSA.

OSU represents an up-scaling procedure that incorporates the area values defined for each pixel as part of a weighted re-sampling scheme. Data are up-scaled to a coarser resolution based on either a user defined value, or a re-sampling heuristic based on the relationship between pixel size, image-objects, and generic point-spread function properties of sensors discussed by Slater (1980).

When OSA is iteratively applied to the resulting mean image, dominant landscape objects start to visually emerge at each new iteration. At the first OSA iteration every pixel is assessed within a progressively growing window until a local *maximum* variance threshold is reached. When this process is applied to the entire image the first image-set (IS_1) is defined, consisting of V_1, A_1, and M_1 (as described above). In the second iteration, each pixel in the newly generated M_1 is assessed until a local *minimum* variance threshold is reached. The resulting images become the second image-set (IS_2) (i.e. V_2, A_2, and M_2) where they represent the beginning scale of all newly emergent image-objects. Thus, odd-numbered OSA iterations define the 'end' of objects, while even-numbered iterations define the beginning of the next emergent object that each pixel is part of. All M_1 generated from even-numbered OSA iterations are then selected for up-scaling. The whole process is iterated until the number of pixels is too small for further processing. Conceptually, this form of processing will eventually result in the entire satellite scene being represented by a single pixel.

The resulting image sets form a nested hierarchy composed of variance, area and mean images that have membership in a unique scale domain (SD_n). Within each SD_n, each image shares the same grain and extent. Furthermore, each SD_n is also a member of a scale-domain super set (SDS) that represents the entire range of OSA and OSU evaluated within a unique satellite image (Hay et al., 2001). In this study, the OSA and OSU framework was applied to Pan_1 and Pan_2. Due to the extent of these images, OSU was conducted four times, resulting in the generation of two SDS. For each SDS, there are five-scale domains associated ($SD_{1–5}$), and for each scale domain, there are two image-sets containing object-specific information (Fig. 4). In total, 30 images were produced that represent the study site through scale.

3.3. Feature detection

Once OSA/OSU processing was completed, MCS is used as a feature detector and applied to the resulting mean images. MCS is a watershed transformation technique that detects regional similarities as opposed to an edge-based technique that detects local changes (Beucher and Lantuéjoul, 1979; Meyer and Beucher, 1990). The key characteristic of MCS is the ability to reduce the problem of over-segmentation found in the original watershed transformation (Roerdink and Meijster, 1999) by placing markers or 'seeds' in user specified areas, from which discrete watershed perimeters can be defined. The general procedure involves three steps:

1. Enhancing variations in image intensity with a gradient operator (i.e. an edge detector) resulting in a gradient image.
2. Defining a relevant marker set and incorporating it into the gradient image.

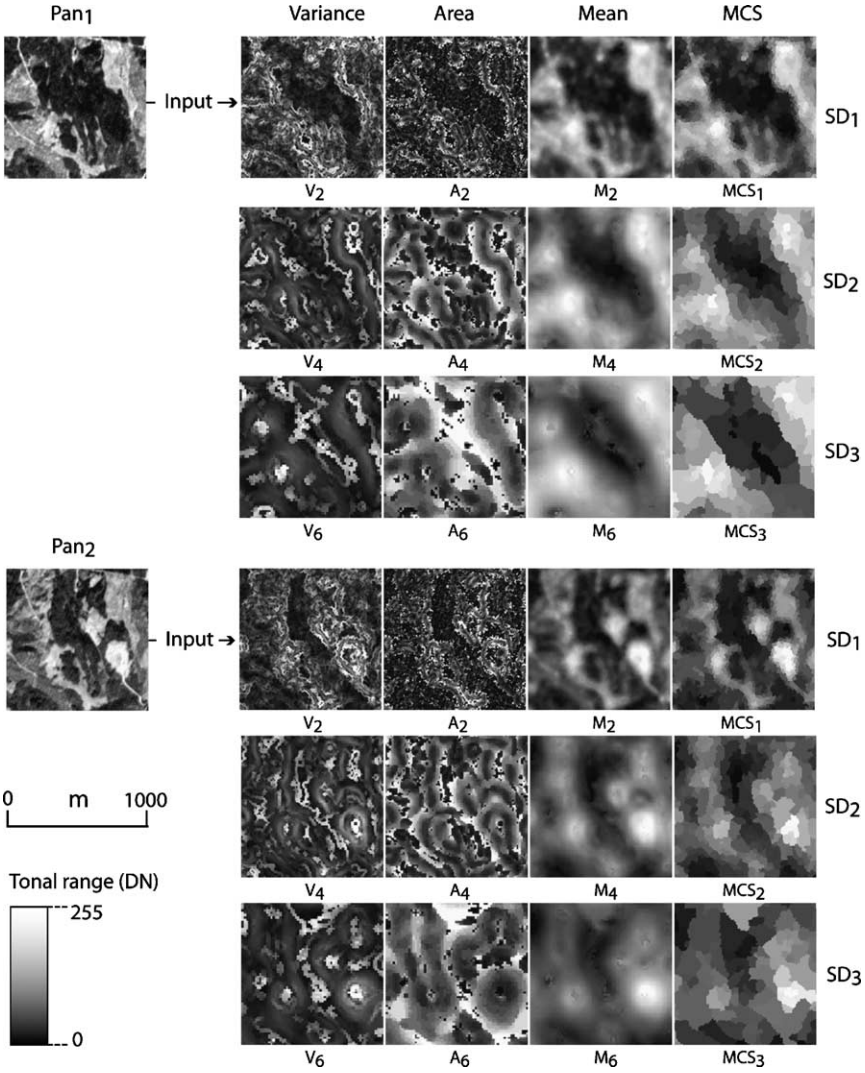

Fig. 4. Multiscale dataset and segmentation images. Note that only a subset of all possible scale domains is represented.

3. Applying the watershed transformation to this modified gradient image.

The elegance of utilizing MCS as a feature detector is that it requires inputs that are automatically and explicitly met by V_I, A_I, and M_I. Specifically, the V_I represents the edges or 'dams' that define individual watersheds in an image. Thus, each even-numbered variance image ($V_{2,4,6,8,10}$) is used as a gradient image. A binary marker set is then obtained automatically by calculating the regional minima on each $A_{2,4,6,8,10}$. These minima are naturally represented by the A_I values due to the low internal variance inherent to image-objects. Each corresponding area and variance image is then combined to represent a modified marker/gradient image. Next, the Matlab watershed algorithm (Vincent and Soille, 1991) is applied to each modified image. This results in 10 new watershed images (5 for Pan_1, 5 for Pan_2), each of which contains closed watershed polygons. Once each polygon is defined, it is labeled with the average of the pixels located with the corresponding M_I, resulting in

topologically discrete watershed image-objects. Fig. 4 illustrates MCS images produced from Pan_1 and Pan_2. In order to distinguish between MCS images of different dates they will be referred to as MCS_{n,Pan_x}, where n indicates the order of MCS processing, and Pan_x indicates the images of origin, i.e. Pan_1 or Pan_2.

3.4. Change detection

The final step involves identifying areas of change in derived datasets. The change detection strategy used here is *image differencing*. Image differencing is a straightforward and commonly used method in remote sensing with the purpose to access the degree of change between two dates on a pixel-by-pixel basis (Dale et al., 1996). A general problem with image differencing is that the maximum difference (in 8-bit data) ranges between −255 to +255, thus the result of the subtraction operation requires scaling to a suitable range (i.e. 0–255). Consequently, no change (i.e. zero value) is replaced with '127'. Values greater than 127 indicate change in one temporal direction, and values below 127 represent change in the opposite direction. Due to its ease in processing and visualization, we have used the absolute (Abs) difference between dates (Eq. (1)):

$$\mathrm{Abs}[Pan_1 - Pan_2] \quad (1)$$

The absolute difference returns the magnitude of change in positive numbers, thus scaling is not

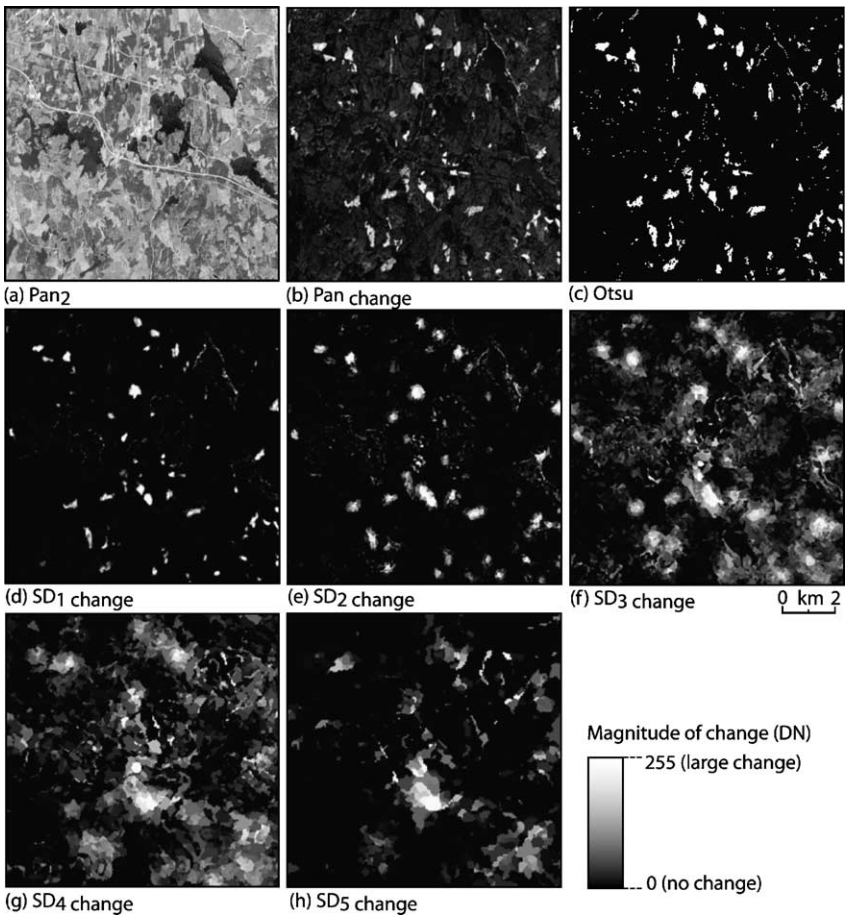

Fig. 5. Change dataset. Note that image (a) represents the original SPOT image, (b and c) represent the change dataset in original scale, and (d–h) represent the multiscale change dataset.

required, and zero indicates no change. The downside of this approach is that the possibility to determine the direction of change is lost. However, this is not a critical factor in this study. A more important task is to establish whether multiscale changes can be detected using MOSA.

We begin by assessing change in the contrast normalized images. To achieve this we apply Eq. (1) to Pan_1 and Pan_2 (output referred to as Pan_{change}), then to $MCS_{1–5,Pan_1}$ and $MCS_{1–5,Pan_2}$ (output referred to as $SD_{1–5,change}$). Note that the results from Pan_1 and Pan_2 (Fig. 5b) contains a gradient of gray-scale change values, i.e. noise + signal, which require further processing to derive discrete change values.

Typically, thresholding is applied to the difference image to define change pixels/objects. However, as noted by Jensen (1996), this requires careful selection of the change/no-change threshold. An absolute difference image tends to elicit a histogram peak located at zero, which tails off rapidly along the *x*-axis. This peak represents pixels that have not changed, while those in the tail represent increased change. The objective is to select a histogram threshold value that discretely separates the 'change' pixels in the image, from non-changed. Unfortunately, image noise resulting from sensor and environmental influences often makes this a non-trivial task.

Thresholding often involves a subjective decision based on a examination of the histogram structure. To reduce this subjectivity, Otsu (1979) proposed a non-parametric and unsupervised method of automatic threshold selection for image segmentation. The optimal threshold is selected based on a discriminant criterion, so as to maximize the separability of the resultant classes in gray levels (for a more in-depth presentation see Otsu, 1979). This algorithm is implemented in the Matlab image processing toolbox and was applied to the difference image in Fig. 5b.

4. Results

Results are presented in two main sections. The first is a description of the MOSA images. Due to the large number (30) of these images, and the need for simplicity in illustration, only the first three scale domains are displayed and discussed. The second section comprises a description of the change detection images.

4.1. MOSA images

The results are displayed in scale domain sets composed of V_I, A_I, M_I, and MCS_I for Pan_1 and Pan_2 (Fig. 4). The variance images represent an 'edge-detection' image. Each pixel in $V_{2,4,6,8,10}$ represents the edge of the image-object under analysis. Bright tones represent high variance (i.e. edges between image-objects), while dark tones represent low variance (i.e. object interiors). Essentially, each pixel in $A_{2,4,6,8,10}$ defines the spatial extent of individual objects as a function of scale. Dark tones indicate that the pixel under analysis is part of an image-object with a small area, while bright tones mean that the pixel belongs to an image-object with a large area. The $M_{2,4,6,8,10}$ images are composed of an average of the high-resolution pixels that constitute part of individual objects assessed at their respective scales. The MCS images represent delineated image-objects based on the object-specific information in V_I and A_I. In each MCS image, all image-objects were labeled with gray tone values derived from the corresponding M_I. To facilitate visual comparison between image-sets, each up-scaled image was re-sampled to the original resolution (1000 × 1000 pixels) using nearest neighbor re-sampling, so that DN values were not changed.

The first image-set, generated at SD_1, has an extent of 1000 × 1000 pixels and grain of 10 m (Table 3). We note that high variance objects (i.e. edges) in the V_2 images correspond to equally bright pixels in A_2 images (i.e. object with large area). At this scale domain, the mean and MCS images appear visually similar. We note in MCS_1, especially in Pan_2, near forest clearings that a diffuse 'zone' is present between the forest and the clearing. The general observation from this scale domain is that many small objects are present.

In SD_2, the number of pixels is reduced to 625 × 625 and the grain has increased to 16 m. As scale increases, visual detail has begun to decline as fewer,

Table 3
Image specific information

SD_n	M_I dimensions	Pixel size (m)	No. of pixels
SD_1	1000 × 1000	10.0	1000000
SD_2	625 × 625	16.0	390625
SD_3	391 × 391	25.6	152881
SD_4	244 × 244	40.9	59536
SD_5	153 × 153	65.5	23409

larger objects dominate the scene. Small roads, observable in SD_1 have disappeared, and nearly all small image-objects have merged into larger structures. We note from V_4 that new 'edges' visually emerge of which only few were observable in SD_1. The M_4 images appear more smoothed, however, the MCS_2 images still reveal many large structures (i.e. image-objects) remain in the scene. The large forest patch in image center (Fig. 4, MCS_{2,Pan_1} shows an almost concentric pattern with many elongated objects surrounding a relatively homogenous interior. We note that in MCS_{2,Pan_2}, the forest clearings at image left have merged into one object and that only one of the former two bright peaks persisted.

The final image set, generated at SD_3, has an extent of 391 × 391 pixels and a grain of 25.6 m. The overall pattern is that fewer, larger objects are formed. In A_{6,Pan_2}, a large homogenous object located in the image center has appeared. This object corresponds to the large forest patch observable at Pan_2. MCS_{3,Pan_2} reveals that on both sides of the forest patch smaller bright objects still persist; in fact, the image is more or less divided in three regions. We note a considerable difference between MCS_{3,Pan_1} and MCS_{3,Pan_2} in overall image structure. In the latter image, few recognizable structures remain, and most of the bright structures have vanished. The forest clearing observable from SD_1 and SD_2 still persist as a visually bright object.

4.2. Change data

Results pertaining to digital change detection will be presented in two sections. The first is a detailed description of the digital change detection capabilities of the MOSA and Otsu (1979) framework at a single scale. The second section is a detailed description of the results from change detection over multiple scales.

4.2.1. Digital change detection in single scale

We begin by assessing the change detection results in the images where grain and extent are the same as in the original dataset (i.e. extent 1000 × 1000 pixels, grain 10 m). This is to validate the framework at a spatial resolution at which our senses are most familiar, thus establishing a precedent for unfamiliar scales where validation is complicated (Granlund and Knutsson, 1995). Results from image differencing are presented in Fig. 5b. Here, a gradient of change is illustrated in gray tones ranging from black (0), which represents no change, through to white (255) representing a large change. We note the presence of many low gray tone change areas. They are most likely due to registration conditions that the normalizing method failed to account for, i.e. atmosphere, and solar angle. We also note the many bright patches, which are the result of clear-cuts and, road construction.

The result from the Otsu (1979) threshold algorithm is presented in Fig. 5c as a binary image where the bright tone indicates 'change' and dark tones 'no change'. Noticeably, most of the low magnitude changes, seen in Fig. 5b, are lost, while changes that coincide with known landscape changes persist. Results show that changes have occurred around some of the lakes in the study site. This is most noticeable in image top right (Fig. 5a and c), which is due to seasonal fluctuation in lake levels. Consequently, more ground is exposed along the lakeshores during the drier months.

The result produced by the Otsu (1979) algorithm (Fig. 5c) is very similar to the result generated by MOSA (Fig. 5d); however, thresholding has not been applied to the MOSA images. Around each dominant MOSA object, there appear to be small border objects with slightly lower gray tone change values. We note that MOSA also identified the aforementioned lakeshore changes. Visually, the change results from MOSA at $SD_{1,change}$ correspond with expectations based on the original SPOT data, and the Otsu threshold algorithm. Therefore, a foundation has been established for the exploration of coarser, less familiar scales.

4.2.2. Multiscale change detection images

With satisfactory results from SD_1, we proceeded to assess the evolution of change through additional scale domains. The entire multiscale change set (i.e. $SD_{1–5,change}$) is presented in Fig. 5d–h. $SD_{1,change}$ was previously described (see above). In $SD_{2,change}$, the grain has increased to 16 m, and the spatial extent has decreased to 625 × 625 pixels. Generally, the same areas in $SD_{1,change}$ are also identified as changed. In addition, a new phenomenon is visible in the image center, where spatially discrete objects appear to connect across the image. Furthermore, a 'fuzzy' edge or zone seems to form around most image-objects. The

gray tone values associated with these edges are generally lower (i.e. darker) than corresponding values for core objects.

The visual impression of $SD_{3,change}$ (Fig. 5f) is very different from the previous scale domains. Here, the spatial extent is 391 × 391 pixels, and the grain has coarsened to 25.6 m. Many of the bright objects from $SD_{1,change}$ still persist, but additional newly changed areas emerge, and in several cases have connected across the image with one or more new objects.

The visual impression from $SD_{4,change}$ is similar to $SD_{3,change}$, although the spatial extent is 244 × 244 pixels and the grain is 40.9 m (Fig. 5g). We note that a few bright patches still persist, especially a large patch in the image center. Many small objects identified at $SD_{3,change}$ have coalesced into larger objects.

The final scale domain (SD_5), exhibits a very different spatial pattern than all previous scale domains. The spatial extent is now 153 × 153 pixels and the grain has reached 65.5 m. We note that the connectedness between the original bright objects from Fig. 5d has decreased and only a few large areas persist. These persisting areas all originate from objects visibly traceable back to $SD_{1,change}$. Most notably, the two forest clearings in the image center continue to persist with high gray tone values preserved. A more detailed illustration of these two objects evolving through scale is found in Fig. 6.

In Pan_{change} (Fig. 6a), two forest clearings are illustrated as bright patches located to the right of image center. Their individual size is approximately 9.4 ha. We also note that the larger forest (dark tone) is identified as changed, visually perceived as dark gray tones. A small road connects one patch with the rest of the road system in the area. In Fig. 6b, this road has vanished together with the minor signals of change. As mentioned earlier, edges are formed around these persisting objects, although spatially small at this scale. At the next scale domain (Fig. 6c), the two forest clearings have coalesced into one object (i.e. 20.5 ha) with a large zone of lower gray values around, approximately 24.4 ha. $SD_{3–5,change}$ is visually very different from previous scale domain (Fig. 6d–f). Generally, no recognizable features are left and the only way to understand the visual pattern is through knowledge of more detailed scales. In essence, larger entities are formed based on the two forest clearings in Fig. 6a.

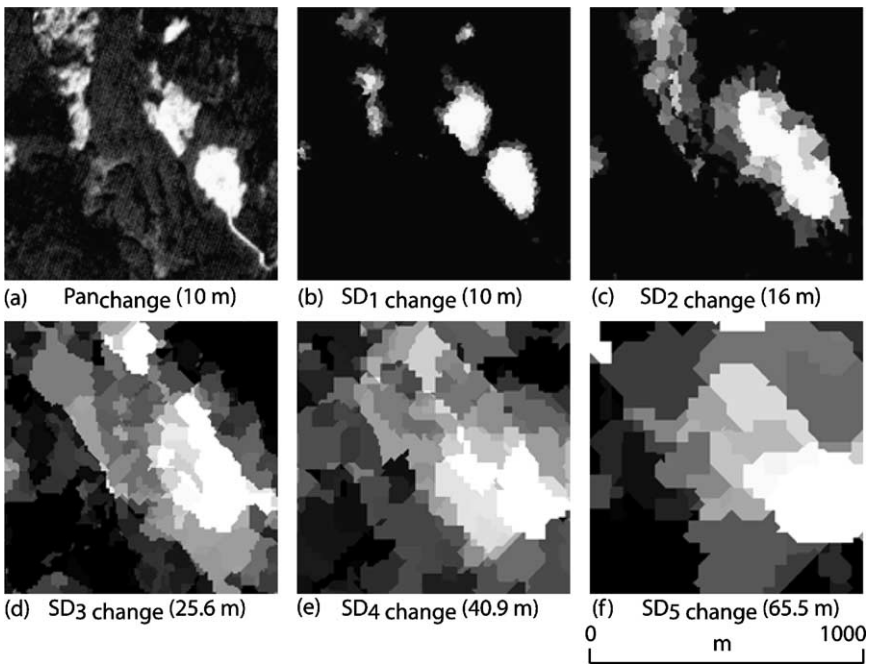

Fig. 6. Detail of multiscale change dataset.

5. Discussion

During the period of investigation (i.e. 1992–1996) active forest practices resulted in many small landscape changes taking place in the study area. By applying an object-specific digital change framework to multitemporal SPOT data dominant landscape changes were identified. Results from detailed scales (SD_1) are consistent with expectations based in the original SPOT data and the Otsu threshold image Figs. 2 and 5c.). Therefore, a foundation for exploration of detailed scales as well as coarser scales is established. Thus, we suggest that image-objects at coarse scales are correct.

5.1. The object-specific approach to digital change detection

An underlying premise of OSA/OSU is that high-resolution image-objects should have more influence on an up-scaled signal than a single bright low-resolution pixel (Hay et al., 2001). In essence, all pixels in a scene are considered high-resolution. This has two consequences for digital change detection. First, we note that sensor related noise, i.e. striping, was effectively ignored by MOSA (Fig. 5d) which is consistent with other multiscale or multiresolution studies (cf. Carvalho et al., 2001). This is a positive effect of the high-resolution pixel concept, as this kind of noise did not have the definitional properties of an image-object. Second, we also note that small features (i.e. a road at $SD_{1,change}$, Fig. 6b) were not defined. The reason is that the same concept did not 'acknowledge' the few pixels that modeled the road as being part of an image-object; instead they were recognized as part of a larger entity (i.e. the surrounding forest). If imagery with a finer spatial resolution were used, i.e. Quickbird or IKONOS Pan data with a spatial resolution of 1 m, the small road would be modeled by more pixels. Thus, the object-specific framework would define and delineate it as an image-object. This is verified in recent work by Hall et al. (2003).

The challenge with marker-controlled segmentation lies in defining which properties to include in the marker set (Beucher, 1992). This is solved within the discussed framework, as V_I, A_I, and M_I are automatically and explicitly included in MCS. Thus, V_I is implemented as a gradient image, a marker set is obtained by calculating the regional minima on A_I, and M_I is used for labeling each watershed polygon with its associated mean spectral value.

The differentiating between 'real' physical landscape changes and changes caused by exogenous factors (i.e. atmospheric conditions), as reported by Fung and LeDrew (1987), Collins and Woodcock (1996) and Carvalho et al. (2001) has not been attempted in this study. Changes caused by differences in atmospheric conditions are more spectrally related, than object related and thus are not likely to affect the V_I and A_I images. Although it is recognized that mean spectral values derived from each M_I that were used for labeling the watershed polygons will be affected by exogenous factors.

The framework described here compares to Deer's (1998) 'feature level' processing. That is, changes are identified and delineated but not labeled with any symbolic meaning. This would require the assistance of a classification algorithm, ancillary data (i.e. forest inventory maps) and additional spectral channels than provided by this study.

5.2. The dynamics of change through scale

The general trend of image-object evolution through scale is that spatially near objects tend to merge into newer, larger objects. Spatially dominant objects tend to persist within one or two scale domains and then suddenly disappear, and new structures emerge at specific scale domains where they did not exist before. This is similar to the scale-space blob events referred to as 'creation', 'merging', and 'annihilation' (Hay et al., 2002). These patterns are visible in Fig. 4 and have been previously reported (for a detailed discussion see, Hall et al., 2003). The same observations are valid for the multiscale change dataset in this study (Fig. 5).

In particular, we find in Figs. 4 and 5, the following two features of special interest: (1) the sudden shift in overall scene composition at specific scale domains, and (2) the formation of 'edges' around evolving image-objects. These features will be discussed in greater detail in the proceeding paragraphs.

1. A drastic shift in overall scene composition is noted between SD_2 and SD_3, and between SD_4 and SD_5.

Hay et al. (2001) reported a similar pattern when OSA/OSU was applied to high-resolution compact airborne spectrographic imager (CASI) data. They suggested that this sudden change was the result of crossing a 'landscape-scale threshold' and used a measure of TSV (total scene variance) for each V_I image in the nested hierarchy. Conceptually, this is the same procedure that is used to calculate the object-specific information in V_I, however, variance is calculated for the *total* of all image-objects defining V_I rather than individual image-objects. The same approach was used by Hall et al. (2003) and applied on IKONOS-2 data. A similar interpretation, in accordance with previous observations, is plausible in this study. The visual appearance of $SD_{1–5}$ indicates that the whole scene is part of a new and larger landscape-object beyond the extent of the study site. This is in agreement with Hierarchy theory, which predicts that changes in spatial pattern are dependent on spatial and temporal scales (Meentemeyer and Box, 1987; Turner, 1989; Malingreau and Belward, 1992).

2. We have noted that when an image-object evolves through scale, most often a zone or, what has been loosely referred to as an 'edge', tend to develop around the objects exterior. This phenomenon is tangible and occupies space, thus Hay et al. (2001) denote the term 'edge-object'. The detailed view in Fig. 6b reveals a thin zone of many small edge-objects around each forest clearing. When we turn to Fig. 6c they have coalesced into one object and we note that the zone now encircles the new image-object. The variance and area images (Fig. 4) indicate that this observation is not limited to the change dataset. A close inspection of the V_I (SD_1) reveals that, at the interface of different vegetation (i.e. forest and clear-cut), a 'double' edge is observable. Corresponding small A_I values indicates that many small objects are formed between these high variance transitions. The apparent question is what do these edge-objects model? Wu and Qi (2002) argue that it is not always certain whether the effect of changing scale is an artifact, or due to the scale multiplicity of landscape systems. Hay et al. (2001) hypothesize that 'edge-objects' represent 'ecotones'. Specifically, they state that edge-objects represent the transition zone between adjacent patches, which could represent small differences in microclimate. Thus edge-objects could be modeling what is known as the *edge-effect* (Chen et al., 1999). For example, around abrupt edges (i.e. around recent clear-cuts) the width of the edge-effect can vary between 60 and 400 m depending on species involved (Chen et al., 1999). According to this hypothesis, the evolution of edge-objects in $SD_{1–5,change}$ models the scale-dependent change occurring within ecotones.

6. Conclusion

Landscapes are complex systems, which can be understood within the theoretical framework of hierarchy theory. This theory predicts that changes in landscape spatial patterns are dependent upon scale specific processes, and the scale at which they are assessed. Remote sensing technology represents the principal tool for obtaining meaningful data on changes in landscapes and MOSA represents a recent approach to generate multiscale data and detect relevant changes with them.

According to the Deer (1998), the framework presented here represents 'feature level processing', thus it is not possible to relate any symbolic meaning to detected objects (Table 1). However, this is only partially correct. Hall et al. (2003) performed a supervised classification on spectrally labeled image-objects of the type found in this study, and reported satisfying results. Consequently, this framework has the ability to perform 'object level processing' with the addition of a standard classification algorithm, thereby enabling symbolic identification of image-objects over multiple scales. Furthermore, the output from this framework is easily represented in either raster and or vector models, for additional analysis within a geographic information system (GIS).

We have reported on an innovative concept that comprises an integration of OSA, OSU and marker-controlled segmentation in an effort to detect landscape changes through multiple scales in SPOT satellite imagery. The result of this is a multiscale change detection framework capable of detecting and delineating relevant changes automatically at their corresponding scale of expression. Results indicate that this framework performs well at the most detailed scale, thus a foundation for exploration of coarser

scales is established. Formal validation of coarser scales remains a challenge for multiscale studies and will continue to be an important subject in future research.

Not until recently have methods been developed to decompose landscape patterns into their constituent multiscale image-objects. Presently, multiscale analysis can be characterized as being in a state where more questions are generated than answered by its use. As we turn our perspective towards unfamiliar scales, our inherent knowledge based on a 'single scale' falls short. As we seek familiarity with new scales recent developments in GIS and spatial statistics (Stein and van der Meer, 2001) will be of vital importance. This study represents one of the first attempts to detect and delineate landscape changes automatically over multiple scales. Such a realization has been identified as an important task in landscape analysis and remote sensing for a number of years (Turner et al., 2001; Lambin, 1996; Turner, 1989).

Acknowledgements

This work has been supported by a scholarship to Dr. Hall by the Foundation for Strategic Environmental Research (MISTRA), by a Natural Sciences and Engineering Research Council (NSERC) postdoctoral research fellowship to Dr. G.J. Hay and by the generous use of the computing facilities, directed by Dr. Danielle Marceau at the Geocomputing Laboratory in the Department of Geography at the University of Montreal, Canada. We also wish to express appreciation to two anonymous referees for their constructive comments.

References

Adams, J.B., Sabol, D.E., Kapos, V., Filho, R.A., Roberts, D.A., Smith, M.O., Gillespie, A.R., 1995. Classification of multispectral images based on fractions of endmembers: application to land cover change in Brazilian Amazon. Remote Sens. Environ. 52, 137–154.

Allen, T.F.H., Starr, T.B., 1982. Hierarchy Perspective for Ecological Complexity. University of Chicago Press, Chicago, 310 pp.

Beucher, S., 1992. The watershed transformation applied to image segmentation. In: Proceedings of the 10th Pfefferkorn Conference on Signal and Image Processing in Microscopy and Microanalysis, Cambridge, UK, 16–19 September 1991. Scann. Microsc. Int. (Suppl. 6), 299–314.

Beucher, S., Lantuéjoul, C., 1979. Use of watersheds in contour detection. In: Proceedings of the International Workshop on Image Processing, Real-time Edge and Motion Detection/ Estimation, CCETT/IRISA Report no. 132, Rennes, France, 17–21 September 1979, pp. 2.1–2.12.

Byrne, G.F., Crapper, P.F., Mayo, K.K., 1980. Monitoring land cover change by principal component analysis of multitemporal Landsat data. Remote Sens. Environ. 10, 175–184.

Carvalho, L.M.T., Fonseca, L.M.G., Murtagh, F., Clevers, J.G.P.W., 2001. Digital change detection with the aid of multiresolution wavelet analysis. Int. J. Remote Sens. 22, 3871–3876.

Chan, J.C.W., Chan, K.-P., Yeh, A.G.-O., 2001. Detecting the nature of change in an urban environment: a comparison of machine learning algorithms. Photogr. Eng. Remote Sens. 67, 213–225.

Chen, J., Saunders, S.C., Crow, T.R., Naiman, R.J., 1999. Microclimate in forest ecosystems and landscape ecology. Bioscience 49, 288–297.

Choo, A., Pham, B., Maeder, A.J., 1989. Change detection in an image sequence using shape analysis. In: Proceedings of the Conference on Image Processing and the Impact of New Technologies, Canberra, 1989, pp. 111–114.

Coiner, J.C., 1980. Using Landsat to monitor changes in vegetation cover induced by desertification processes. In: Proceedings of the 14th International Symposium on Remote Sensing Environment, Ann Arbor, MI, 1980.

Collins, J.B., Woodcock, C.E., 1994. Change detection using the Gramm-Schmidt transformation applied to mapping forest mortality. Remote Sens. Environ. 50, 267–279.

Collins, J.B., Woodcock, C.E., 1996. An assessment of several linear change detection techniques for mapping forest mortality using multitemporal Landsat TM data. Remote Sens. Environ. 56, 66–77.

Coppin, P.R., Bauer, M.E., 1994. Processing of multitemporal Landsat TM imagery to optimize extraction of forest cover change features. Geosci. Remote Sens. 60 (3), 287–298.

Dai, X., Khorram, S., 1997. Development of new automated land cover change detection system from remotely sensed imagery based on artificial neural networks. In: Proceedings of the 1997 International Geoscience Remote Sensing Symposium (IGARSS 97), 1997, pp. 1029–1031.

Dai, X., Khorram, S., 1998. The effects of image misregistration on the accuracy of remotely sensed change detection. IEEE Trans. Geosci. Remote Sens. 36, 1566–1577.

Dale, P.E.R., Chandica, A.L., Evans, M., 1996. Using image subtraction and classification to evaluate change in sub-tropical inter-tidal wetlands. Int. J. Remote Sens. 17, 703–719.

Daubechies, I., 1988. Orthonormal bases of compactly supported wavelets. Commun. Pure Appl. Math. 41, 906–966.

Deer, P., 1998. Digital change detection in remotely sensed imagery using fuzzy set theory. Ph.D. thesis, Department of Geography and Department of Computer Science, University of Adelaide, Australia.

Deer, P., Eklund, P., 2001. Fuzzy Logic for Change Detection in Classified Images. Fuzzy Logic and Soft Computing Series, Springer-Verlag, Berlin.

Deer, P.J., Longmore, M.E., 1994. The application of principal components analysis to monitoring the clearance of native forest stands on Kangaroo island, South Australia. In: Proceedings of the 7th Australasian Remote Sensing Conference, Melbourne, Australia, 1994.

Eklund, P., You, J., Deer, P., 2000. Mining remote sensing image data: an integration of fuzzy set theory and image understanding techniques for environmental change. Proc. SPIE 2000, 66–67.

Fisher, P.F., Pathirana, S., 1993. The ordering of fuzzy land cover information derived from Landsat MSS data. Geocarto Int. 3, 5–14.

Foody, G.M., 2001. Monitoring the magnitude of land cover change around the southern limits of the Sahara. Photogr. Eng. Remote Sens. 67, 841–847.

Fung, T., LeDrew, E., 1987. The application of principal components analysis to change detection using various accuracy indices. Photogr. Eng. Remote Sens. 53, 1649–1658.

Gong, P., LeDrew, E.F., Miller, J.R., 1992. Registration–noise reduction difference images for change detection. Int. J. Remote Sens. 13, 773–779.

Gopal, S., Woodcock, C., 1996. Remote sensing of forest change using artificial neural networks. IEEE Trans. Geosci. Remote Sens. 34, 398–404.

Gordon, S., 1980. Utilizing Landsat imagery to monitor land use change. Remote Sens. Environ. 9, 189–196.

Granlund, G.H., Knutsson, H., 1995. Signal Processing for Computer Vision. Kluwer Academic Publishers, Dordrecht, p. 437.

Hall, O., 2002. Landscape from space: geographical aspects on scale, regionalization and change detection. Meddelanden No. 16, Department of Human Geography, Stockholm University, p. 101, ISBN 91-7265-576-3.

Hall, O., Hay, G.J., Marceau, D., Bouchard, A., 2003. Detecting landscape objects through multiple scales: an integration of object-specific methods and watershed segmentation. Landsc. Ecol., submitted for publication.

Hanaizumi, H., Okumura, H., Fujimura, S., 1991. Change detection from remotely sensed multitemporal images using spatial segmentation. In: Proceedings of the 1991 International Geoscience Remote Sensing Symposium (IGARSS 91), 1991, pp. 1079–1081.

Hay, G.J., Niemann, K.O., 1994. Visualizing 3-D texture: a three-dimensional structure approach to model forest texture. Can. J. Remote Sens. 20 (2), 90–101.

Hay, G.J., Niemann, K.O., McLean, G., 1996. An object-specific image-texture analysis of H-resolution forest imagery. Remote Sens. Environ. 55, 108–122.

Hay, G.J., Niemann, K.O., Goodenough, D.G., 1997. Spatial thresholds, image-objects and up-scaling: a multiscale evaluation. Remote Sens. Environ. 62, 1–19.

Hay, G.J., Marceau, D.J., Bouchard, A., Dubé, P., 2001. A multiscale framework for landscape analysis: object-specific up-scaling. Landsc. Ecol. 16, 471–490.

Hay, G.J., Dubé, P., Bouchard, A., Marceau, D.J., 2002. A scale-space primer for exploring and quantifying complex landscapes. Ecol. modell. 153, 27–49.

Hay, G.J., Blaschke, T., Marceau, D.J., Bouchard, A., 2003. A comparison of three image-object methods for the multiscale analysis of landscape structure. ISPRS J. Photogr. Remote Sens. 57 (5–6), 327–345.

Hoffer, R.M., Lee, K.S., 1989. Forest change classification using SEASAT and SIR-B satellite SAR data. In: Proceedings of the 1989 International Geoscience Remote Sensing Symposium (IGARSS 89), 1989, pp. 1372–1375.

Holling, C.S., Gunderson, L.H., Ludwig, D., 2002. In quest for a theory of adaptive change. In: Gunderson, L.H., Holling, C.S. (Eds.), Panarchy. Understanding Transformations in Human and Natural Systems. Island Press, pp. 3–22.

Hu, Z., Chen, Y., Islam, S., 1998. Multiscaling properties of soil moisture images and decomposition of large- and small-scale features using wavelet transforms. Int. J. Remote Sens. 19, 2451–2467.

Jansson, U., 2001. Regioner i Örebro län. Opublicerad rapport vid Länsstyrelsen i Örebro, in Swedish.

Jensen, J.R., 1996. Digital change detection. In: Introductory Digital Image Processing, second ed. Prentice-Hall, New Jersey, pp. 257–277 (Chapter 3).

Jensen, J.R., Rutchey, K., Koch, M.S., Narumalani, S., 1995. Inland wetland change detection in the Everglades water conservation area 2A using time series of normalized remotely sensed data. Photogr. Eng. Remote Sens. 61, 199–209.

Jha, C.S., Unni, N.V.M., 1994. Digital change detection of forest conversion of a dry tropical forest region. Int. J. Remote Sens. 15, 2543–2552.

Johnson, R.D., Kasischke, E.S., 1998. Change vector analysis: a technique for the multispectral monitoring of land cover and condition. Int. J. Remote Sens. 19, 411–426.

Klinger, A., 1971. Pattern and search statistics. In: Rustagi, J.S. (Ed.), Optimizing Methods in Statistics. Academic Press, New York, pp. 303–339.

Klinger, A., Dyer, C.R., 1976. Experiments in picture representation using regular decomposition. Comput. Graph. Image Process. 5, 68–105.

Kressler, F.P., Steinnocher, K.T., 1999. Detecting land cover changes from NOAA AVHRR data by using spectral mixture analysis. Int. J. Appl. Earth Observ. Geoinform. 1, 21–26.

Lambin, E.F., 1996. Change detection and multitemporal scales: seasonal and annual variations in landscape variables. Photogr. Eng. Remote Sens. 62, 931–938.

Lambin, E.F., Strahler, A.H., 1994. Change vector analysis in multitemporal space: a tool to detect and categorise land cover change processes using high temporal resolution satellite data. Remote Sens. Environ. 48, 231–244.

Lazaroff, M.B., Brennan, M.W., 1992. Multitemporal texture analysis of features computed from remotely sensed imagery. Proc. SPIE 1819, 166–175.

Lindeberg, T., 1994. Scale-space theory: a basic tool for analyzing structures at different scales. J. Appl. Stat. 21 (2), 225–270.

Lodwick, G.D., 1979. Measuring ecological changes in multitemporal Landsat TM data using principal components. In: Proceedings of the 13th International Symposium on Remote Sensing Environment, Ann Arbor, MI, 1979, pp. 1131–1141.

Lyon, J.G., Yuan, D., Lunetta, R.S., Elvidge, C.D., 1998. A change detection experiment using vegetation indices. Photogr. Eng. Remote Sens. 64, 143–150.

Malila, W.A., 1980. Change vector analysis: an approach for detecting forest change with Landsat. In: Proceedings of the Annual Symposium on Machine Processing of Remotely Sensed Data, IEEE, 1980, pp. 326–336.

Malingreau, J.P., Belward, A.S., 1992. Scale considerations in vegetation monitoring using AVHRR data. Int. J. Remote Sens. 13, 2289–2307.

Manavalan, P., Kesavasamy, K., Adiga, S., 1995. Irrigated crops monitoring through seasons using digital change detection analysis of IRD-LISS 2 data. Int. J. Remote Sens. 16, 633–640.

Mandelbrot, B., 1967. The fractal geometry of nature. Science 156, 636–642.

Marceau, D.J., 1999. The scale issue in the social and natural sciences. Can. J. Remote Sens. 25 (4), 347–356.

Marceau, D.J., Hay, G.J., 1999. Remote sensing contributions to the scale issue. Can. J. Remote Sens. 25 (4), 357–366.

Matsuyama, T., 1987. Knowledge-based aerial image understanding systems and expert systems for image processing. IEEE Trans. Geosci. Remote Sens. 25, 305–316.

Meentemeyer, V., 1989. Geographical perspectives of space, time, and scale. Landsc. Ecol. 3 (3–4), 163–173.

Meentemeyer, V., Box, E.O., 1987. Scale effects in landscape studies. In: Turner, M.G. (Ed.), Landscape Heterogeneity and Disturbance. Springer-Verlag, Berlin, pp. 15–34.

Meyer, F., Beucher, S., 1990. Morphological segmentation. J. Visual Commun. Image Represent. 1 (1), 21–46. Academic Press, New York.

Munyati, C., 2000. Wetland change detection on the Kafue Flats, Zambia, by classification of a multitemporal remote sensing image dataset. Int. J. Remote Sens. 21, 1787–1806.

Nelson, R.F., 1983. Detecting forest canopy change due to insect activity using Landsat MSS. Photogr. Eng. Remote Sens. 49, 1303–1314.

Openshaw, S., 1984. The modifiable areal unit problem. Concepts Tech. Mod. Geogr. (CATMOG) 38, 40.

Otsu, N., 1979. A threshold selection method from gray-level histograms. IEEE Trans. Syst. Man Cybernet. 9 (1), 62–66.

Riordan, C.J., 1980. Non-urban to urban land cover change using Landsat data. Summary report of the Colorado Agricultural Research Experiment Station, Fort Collins, CO.

Roerdink, J.B.T.M., Meijster, A., 1999. The watershed transform: definitions, algorithms and parallelization techniques. Institute for Mathematics and Computer Science, University of Groningen, Groningen, The Netherlands, IWI 99-9-06, 1999.

Schott, J.R., Salvaggio, C., Volchok, W.J., 1988. Radiometric scene normalization using pseudo-invariant features. Remote Sens. Environ. 26, 1–16.

Serra, J., 1988. Image Analysis and Mathematical Morphology. II. Theoretical Advances. Academic Press, London.

Siljeström Ribed, P., Moreno Lópes, A., 1995. Monitoring burnt areas by principal components analysis of multitemporal TM data. Int. J. Remote Sens. 16 (9), 1577–1587.

Singh, A., 1986. Change detection in the tropical forest environment of northeastern India using Landsat. In: Eden, M.J., Parry, J.T. (Eds.), Remote Sensing and Tropical Land Management, Wiley, Chichester, pp. 237–254.

Singh, A., 1989. Digital change detection techniques using remotely-sensed data. Int. J. Remote Sens. 10, 989–1003.

Singh, A., Harrison, A., 1985. Standardized principal components. Int. J. Remote Sens. 6, 883–896.

Slater, P.N., 1980. Remote Sensing: Optics and Optical Systems. Addison-Wesley, Reading, MA, 575 pp.

Song, C., Woodcock, C.E., Seto, K.C., Pax Lenney, M., Macomber, S.A., 2001. Classification and change detection using Landsat TM data: when and how to correct atmospheric effects? Remote Sens. Environ. 75, 230–244.

Starck, J.L., Murtagh, F., Bijaoui, A., 1998. Image Processing and Data Analysis: The Multiscale Approach. Cambridge University Press, Cambridge, 285 pp.

Stefanov, W.L., Ramsey, M.S., Christensen, P.H., 2001. Monitoring urban land cover changes: an expert system approach to land cover classification of semiarid to arid urban centers. Remote Sens. Environ. 77, 173–185.

Stein, A., van der Meer, F., 2001. Statistical sensing of the environment—space, time, scale: combining remote sensing and spatial statistics for ecology and the environment. Int. J. Appl. Earth Observ. Geoinform. 3 (2), 111–113.

Todd, W.J., 1977. Urban and regional land use change detected by using Landsat data. J. Res. United States Geol. Surv. 5, 527–534.

Townshend, J.R.G., Justice, C.O., 1988. Selecting the spatial resolution of satellite sensors required for global monitoring of land transforms. Int. J. Remote Sens. 9, 187–236.

Turner, M.G., 1989. Landscape ecology: the effect of pattern on process. Annu. Rev. Ecol. Systemat. 20, 171–197.

Turner, M., Gardner, R.H., O'Neill, R.V., 2001. Landscape Ecology in Theory and Practice. Springer-Verlag, New York, 375 pp.

Vincent, L., Soille, P., 1991. Watersheds in digital spaces: an efficient algorithm based on immersion simulations. IEEE Trans. Pattern Anal. Mach. Intell. 13 (6), 125–583.

Virag, L.A., Colwell, J.E., 1987. An improved procedure for analysis of change in thematic mapper image-pairs. In: Proceedings of the 21st International Symposium on Remote Sensing Environment, Ann Arbor, MI, 1987.

Weismiller, R.A., Kristof, S.J., Scholz, P.E., Anuta, P.E., Momin, S.A., 1977. Change detection in coastal zone environments. Photogr. Eng. Remote Sens. 43, 1533–1539.

Wiens, J.A., 1989. Spatial scaling in ecology. Funct. Ecol. 3, 385–397.

Woodcock, C.E., Strahler, A.H., 1987. The factor of scale in remote sensing. Remote Sens. Environ. 21, 311–332.

Wu, J., Qi, Y., 2002. Dealing with scale in landscape analysis: an overview. Geogr. Inform. Sci. 6 (1), 1–5.

Yang, X., Lo, C.P., 2000. Relative radiometric normalization performance for change detection from multidate satellite images. Photogr. Eng. Remote Sens. 66 (8), 967–980.